3830 *Macromolecules* **2009**, *42*, 3830–3840
DOI: 10.1021/ma9003743

Macromolecules
PERSPECTIVE

A Case for Characterizing Polymers with the Kerr Effect

Alan E. Tonelli*

Fiber & Polymer Science Program, North Carolina State University, Campus Box 8301, Raleigh, North Carolina 27695-8301

Received February 18, 2009; Revised Manuscript Received April 14, 2009

ABSTRACT: We briefly summarize Kerr effect studies of dilute polymer solutions, taken from our own work, for the purpose of emphasizing their unique ability to characterize polymer microstructures. In cases where at least one of their monomer repeat units is polar or at least reasonably and anisotropically polarizable, the molar Kerr constants, ${}_mK$, of polymers obtained from the electrical birefringence measured for their dilute solutions are demonstrated to be exquisitely sensitive to their microstructures, including the tacticities of homo- and copolymers and the comonomer sequences of copolymers. In addition, because the ${}_mK$s expected for polymers with given or known microstructures can be calculated if their conformational characteristics have been established, comparison of observed and calculated ${}_mK$s can also be used to confirm or derive their conformational characteristics, such as those embodied in their rotational isomeric states (RIS) models. From such comparisons of observed and calculated ${}_mK$s, we were able to conclude that, among all characterization techniques, Kerr effect studies of dilute polymer solutions are clearly the most sensitive to both their microstructures and their conformations. This is largely a consequence of the fact that the ${}_mK$s of small molecules range over more than 4 orders of magnitude and, in addition, may be either positive or negative in sign. Several additional potential applications of the Kerr effect are suggested for polymers that interact/complex with each other or with certain small molecules in solution and also for polymers at interfaces, e.g., polymer brushes bathed/swollen in solvents. Finally a call (a plea really) is made for polymer samples containing polar or anisotropically polarizable repeat units for further evaluating the Kerr effect as a sensitive means to characterize both their microstructures and conformations. This request is made because of our soon to be achieved and unique capability to measure ${}_mK$s of polymers in solution on a state-of the-art Kerr effect instrument nearing completion in our laboratory.

Introduction

Though biopolymers have always been central to life, only relatively recently have materials made from synthetic polymers become dominant in our society. While the detailed microstructures of biopolymers, and, as a consequence, their functions, are far more complicated and diverse than those of synthetic macromolecules, they are at the same time more readily elucidated. For example, the $\sim(20)^{100}$ potentially distinct proteins containing 100 amino acids may each be distinguished by reading the genetic code of the DNA used in their syntheses.[1] On the other hand, the microstructural analyses of free-radically synthesized vinyl polymers, such as methyl methacrylate (M)/styrene (S) copolymers (poly-M/S), for example, seem to be beyond our current capabilities.[2−4] When both the stereo- and comonomer sequences are considered, there are 20 possible distinct M/S comonomer triads[2,3] [M-(r or m)-M-(r or m)-M, M-(r or m)-S-(r or m)-M, S-(r or m)-S-(r or m)-M, ..., S-(r or m)-S-(r or m)-S.] Because there exists no readable template for their syntheses, microstructural analyses of M/S copolymers require identification of all 20 possible distinct M/S triads as they occur post-polymerization in poly(M/S) chains.

This is well beyond the capability of the currently most sensitive technique for determining polymer microstructures, solution ^{13}C NMR spectroscopy,[2−4] because distinct resonances cannot be observed for each, or even a majority, of the 20 comonomer triads in poly(M/S). The inability of solution ^{13}C NMR to discriminate between the microstructures of polymers is not limited to chain-growth polymers but is also evident when applied to step-growth polymers, such as polyester and polyamide copolymers. Take the hypothetical copolyester made with ethylene glycol (EG) and the diacids, 1,4-butanedioic (B) and 1,8-octanedioic (O) acids, for example. ^{13}C NMR would likely be unable to distinguish even between their comonomer diad sequences, ...B-EG-B..., ...B-EG-O..., and ...O-EG-O.... Even though the methylene and carbonyl resonances of the B and O diacid fragments would be expected to be unique, it is unlikely their resonance frequencies would be sensitive to the chemical nature (B or O) of their nearest-neighbor diacids attached across common EG fragments because both their nearby substituent groups and local conformations are unaffected by whether or not they have B or O neighbors.[2]

This prompts the question, are there any experimental means available to determine the microstructures of polymers that can potentially overcome the inherent shortcomings of even the presently best method, NMR spectroscopy? I believe the answer is yes, and surprisingly the technique is one that "macroscopically" probes the complete macromolecule and not just its local microstructure, as NMR does spectroscopically. The electrical birefringence or Kerr effect measured for dilute polymer solutions has the potential to be sensitive to, reflect, and characterize much longer-range microstructures in polymers containing repeat units that are polar or substantially and anisotropically polarizable.

Belief in the Kerr effect as a potentially sensitive means to characterize polymer microstructures was recently rekindled and supported by the observed insensitivity of NMR stectroscopy to the comonomer sequences in atactic-styrene/*p*-Br-styrene

*E-mail: alan_tonelli@ ncsu.edu.

 Published on Web 05/13/2009

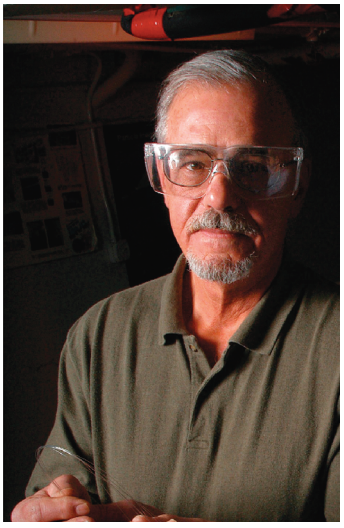

Alan Tonelli received a B.S. in Chemical Engineering from the University of Kansas in 1964 and a Ph.D. in Polymer Chemistry from Stanford in 1968, where he was associated with the late Professor Paul J. Flory. He was a member of the Polymer Chemistry Research Department at AT&T-Bell Laboratories, Murray Hill, NJ, for 23 years and in 1991 joined the Fiber & Polymer Science Program in the College of Textiles at North Carolina State University in Raleigh, NC, where he is currently the INVISTA Professor of Fiber and Polymer Chemistry. His research interests include the configurations, conformations, and structures of synthetic and biological polymers, their determination, principally by NMR and Kerr effect observations, and establishing their effects on the physical properties of polymer materials. Most recently, the formation of and coalescence from noncovalent crystalline inclusion compounds (ICs) formed between cyclodextrin (CD) hosts and polymer guests have been used to nanostructure bulk polymers, including homopolymers and their blends, and block copolymers. In addition, small-molecule guest−CD−ICs (crystalline) and −rotaxanes (soluble), and the covalent incorporation of CDs into polymers both during and subsequent to their syntheses, have been used to improve the delivery of additives to polymer materials.

(S/*p*-BrS) copolymers. As subsequently described, the NMR spectra of S/*p*-BrS copolymers are distinguishable only by the resonant frequencies of their aromatic carbons. Consequently, the only information they provide is the overall comonomer composition but provide no information concerning the distribution of S and *p*-BrS units, i.e., their comonomer sequence distribution.

Here we attempt to make the case for improving the microstructural characterization of polymers by comparing the molar Kerr constants, ${}_{\mathrm{m}}K$s, measured in their dilute solutions to those estimated based on their conformational characteristics, in conjunction with the dipole moments and polarizabilities of their constituent bonds. Because no electrical birefringence studies of dilute polymer solutions have been reported for more than a decade and because we are currently building a state-of-the-art instrument to do so, we are asking polymer scientists interested in improving the microstructural characterization of their polymers to collaborate with us by examining them with the Kerr effect. In addition, we suggest several new applications of the Kerr effect to investigate both the interactions between polymers (self and mutual) and with small molecules and the nature of polymer brushes.

The Kerr Effect

Theory. When a strong electromagnetic field is applied to an initially isotropic material, its constituent molecules are induced to align, as a consequence of their inherent polarities and polarizabilities, and the material is rendered anisotropic. In the presence of the strong electromagnetic field, E, the material evidences a birefringence, Δn, because its refractive index now depends on direction and may be either larger or smaller parallel to, $n_{\|}$, than perpendicular to, $n_{\perp}$, the applied field. In 1875, John Kerr[5] first observed that the birefringence, $\Delta n = n_{\|} - n_{\perp}$, induced by the applied electric field E in both solids and liquids scales as $(B/\lambda)E^2$, where λ is the wavelength of light employed to measure the refractive indices and B is the Kerr constant.

In solutions,[6−10] the Kerr constant B_{12} is contributed to by the E field alignment of both the solvent (1) and solute molecules (2), with volume fractions $\varphi_{1,2}$. Thus, $B_{12} = B_1\varphi_1 + B_2\varphi_2 = B_1 - B_1\varphi_2 + B_2\varphi_2$, and so the Kerr constant of the solute $B_2 = \Delta B/\varphi_2 + B_1$, where ΔB is the difference between the Kerr constants of the solution (12) and the solvent (1), with the former extrapolated to infinite dilution. Whether or not the alignment of solvent and solute molecules are dominated by their permanent dipole moments or those induced in them by the strong E field, their Kerr constants, Bs, i.e., their contributions to the induced birefringence, depend on both their molecular dipole moments and anisotropic polarizabilities. For flexible polymers in solution, this means their contribution to the electrical birefringence depends on their macroscopic molecular dipole moments and polarizabilities averaged over all the conformations they are rapidly sampling.

Nagai and Ishikawa[11] first developed the formal expressions relating the overall molecular dipole moments and polarizability tensors of flexible polymers to yield the relation connecting the birefringence they produce at infinite dilution in solution (molar Kerr constant, ${}_{\mathrm{m}}K$, subsequently discussed) in response to their alignment by the electric field E.

$$ {}_{\mathrm{m}}K = (2\pi N_{\mathrm{A}}/135)[(\langle \mu^{\mathrm{T}}\alpha\mu\rangle)/k^2T^2 + (\langle \mathrm{tr}(\alpha^{\mathrm{R}}\acute{\alpha}^{\mathrm{C}})\rangle)/kT] $$

where N_{A} and k are the Avogadro and Boltzmann constants and T is the temperature. μ^{T}, μ are the overall polymer dipole moment vectors expressed as a row,column, α, α^{R} and $\acute{\alpha}^{\mathrm{C}}$ are the overall anisotropic optical and static polarizability tensors of the polymer, with both contributing to $\Delta\alpha$, the difference in polarizabilities of the entire polymer chain in directions parallel and perpendicular to the applied field E. α and $\acute{\alpha}$ are both traceless, and the superscripts R and C denote their row and column forms. Finally, $\langle\,\rangle$ indicates an average over all conformations available to the polymer.

Flory and Jernigan[12−14] subsequently demonstrated how matrix multiplication techniques can be applied to the dipolar $\langle \mu^{\mathrm{T}}\alpha\mu\rangle$ and polarizability $\langle \mathrm{tr}(\alpha^{\mathrm{R}}\acute{\alpha}^{\mathrm{C}})\rangle$ terms of the Nagai−Ishikawa expression to perform the correct averaging of both over all of the realistic rotational isomeric state (RIS) conformations available to flexible polymer chains. Critical to its implementation is the assumption of constituent bond dipole moments and polarizability tensors that are both additive and independent of conformation. This permits a comparison of realistically calculated and experimentally observed molar Kerr constants for polymers, which, as we shall soon see, can be important to the determination of their microstructures. However, we now turn to the experimental evaluation of the molar Kerr constants, ${}_{\mathrm{m}}K$s, of solutes obtained from the birefringence induced in their dilute solutions by application of strong electric fields.

Experiment. In addition to their many Kerr effect studies of polymers in solution, Riande and Saiz[15] have provided a nice summary of the experimental determination and theoretical calculation of their molar Kerr constants ${}_{\mathrm{m}}K$. For all but the most isotropic (nonpolar and minimally polarizable) polymers, the molar Kerr constant of the

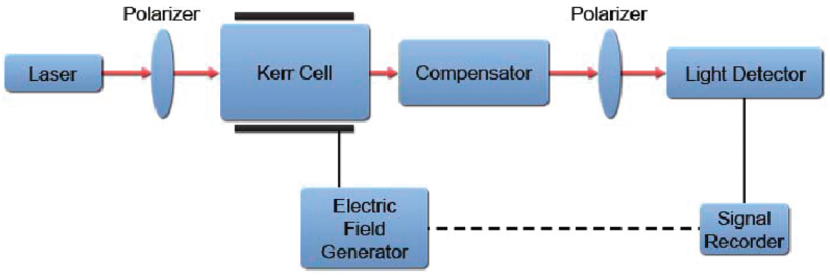

Figure 1. Schematic of a typical Kerr effect instrument.

polymer solute obtained at infinite dilution in isotropic solvents may be experimentally determined[16,17] with the following relation:

$$_{\mathrm{m}}K = (6N_{\mathrm{A}}\lambda nB)/[\rho(n+2)^2(\varepsilon+2)^2]$$

where n, B, ρ, and ε are the refractive index, Kerr constant, density, and dielectric constant of the polymer solution, all extrapolated to infinite dilution. A schematic diagram of the components essential for Kerr effect measurements is presented in Figure 1. A refractometer operating at the same wavelength as the Kerr effect instrument and a dielectric meter are also necessary components for measuring the required refractive indices and dielectric constants of the dilute polymer solutions.

In addition, because measurement of the dielectric constants of the polymer solutions are required for evaluation of $_{\mathrm{m}}K$, we may also extract from them the dipole moments, $\langle\mu^2\rangle$, of the dissolved polymer chains. With knowledge of a polymer's RIS conformational description and constituent bond dipole moments, and matrix multiplication techniques analogous and identical to those[13] used to calculate its molar Kerr constant and dimensions ($\langle r^2\rangle$), the mean-square dipole moments averaged over all conformations may also be calculated. This provides an additional property potentially useful for characterizing the microstructures and conformations of polymers. However, as will soon become apparent, $_{\mathrm{m}}K$ is much more sensitive than $\langle\mu^2\rangle$ to both of these fundamental characteristics of flexible polymers.

Kerr Effect Studies of Polymers

In 1977, the molar Kerr constants expected for a variety of vinyl homo- and copolymers were calculated,[18] as outlined above, and found to display a remarkable sensitivity to both their tacticities and comonomer sequences when at least some of their monomer units were polar. This prompted a series of experimental Kerr effect studies,[19−26] where $_{\mathrm{m}}K$s were measured on dilute solutions of a variety of polymers and oligomers and compared successfully to their calculated values. These studies demonstrated that the electrical birefringence contributed by individual polymers to the Kerr effects measured for their dilute solutions could be used to characterize both their microstructures and conformations. In the following, we briefly highlight portions of these studies.

PEO. Molar Kerr constants were measured[19,20] for poly(ethylene oxide) (PEO) in solution as a function of their molecular weights, their modes of termination (−OH and $-OCH_3$), and the solvents used. They were found to agree with those estimated using the RIS conformational model appropriate to PEO and assuming additivity of their bond polarizabilities and dipole moments. It should be emphasized that this agreement was achieved despite the fact that experimentally their $_{\mathrm{m}}K$s per repeat unit were not very different from CCl_4, one of the isotropic solvents used for their measurement. Also, similar $_{\mathrm{m}}K$s were obtained in CCl_4, cyclohexane, and dioxane, indicating the absence of excluded volume/solvent quality effects on the Kerr effect, which have to be addressed when measuring their dimensions ($\langle r^2\rangle$), for example. For PEO both the dipolar and polarizabilty[27] terms contributed significantly to the calculated $_{\mathrm{m}}K$s, but with negative and positive contributions, respectively.

Additionally, when previously measured in the anisotropic solvent benzene, much larger $_{\mathrm{m}}K$s were obtained.[30] It was suggested[20] that this was caused by specific solvation of the PEO chains through close association of the anisotropic benzene molecules. This suggests that the Kerr effect of polymers may be sensitive to their interactions in solution with small molecules and by analogy to those with other polymers. Furthermore, the noncovalent complexation of small molecules in solution should likewise benefit from Kerr effect studies, which should be sensitive to both their degrees of and modes of complexation/interaction. Each of these potential applications of the Kerr effect to study molecular interactions in solution will be subsequently discussed.

α,ω-Dibromoalkanes. Molar Kerr constants and dipole moments were measured in cyclohexane for a series of α,ω-dibromoalkanes [$Br-(CH_2)_n-Br$, with $n = 3-20$].[20] While $\langle\mu^2\rangle$s were observed to increase gradually with n by a factor of ∼2, $_{\mathrm{m}}K$s of −4.5 to 160 ($\times 10^{-12}$ cm^7 S C^{-2} mol^{-1} or cm^5 statvolts^{-2} mol^{-1}) were measured for $n = 3-20$. With increasing n, the observed $\langle\mu^2\rangle$s and $_{\mathrm{m}}K$s gradually tapered off to twice the values observed for ethyl bromide. This demonstrated that the relative positions and orientations of the terminal Br—α-CH_2− and −ω-CH_2—Br bonds lose their conformational correlation when separated by ∼15 intervening $-CH_2-CH_2-$ bonds, which may be identified with the Kuhn length[31] appropriate for long n-alkanes, including polyethylene.

In addition, structural and additional conformational information was derived from a comparison of observed and calculated $_{\mathrm{m}}K$s, which were found to agree, with the latter dominated by the dipolar term ($\langle\mu^{\mathrm{T}}\alpha\mu\rangle$). First, agreement was best if the direction of the $-CH_2-Br$ dipole moment was displaced from the −C—Br bond. Second, quantitative agreement was only possible if the gauche± ($g^{\pm}$) conformations permitted to the first and last $-CH_2-CH_2-$ bonds were assumed to be ±(80°−90°), rather than the usual perfectly staggered values of ±120° (trans = t = 0°). This displacement away from the perfectly staggered gauche± conformations is the expected[24] response to reducing the steric repulsion between bulky Br atoms and CH_2 groups separated by three bonds.

Fluoropolymers. The $_{\mathrm{m}}K$s and $\langle\mu^2\rangle$s of three fluoropolymers [poly(fluoromethylene (PFM) = $-(CHF)_x-$, poly(vinylidene fluoride (PVF_2) = $-(CF_2-CH_2)_x-$, and poly(trifluoroethylene) (PVF_3) = $-(CHF-CF_2)_x-$] were measured[24] in *p*-dioxane with the results presented in Table 1. Their $_{\mathrm{m}}K$s and $\langle\mu^2\rangle$s are both seen to vary by an order of

Table 1. Experimental Molar Kerr Constants and Dipole Moments of Fluoropolymers per Repeat Unit *x*

	$({}_mK/x)^a$	$(\langle\mu^2\rangle/x)^b$
$PVF_3 = -(CHF-CF_2)_x-$	−9.1	0.86
$PFM = -(CHF)_x-$	∼0	0.31
$PVF_2 = -(CF_2-CH_2)_x-$	14	2.38

$^a \times 10^{-12}$ cm^7 S C^{-2} mol^{-1}. $^b \times 10^{-36}$ cm^2 S C^2 mol^{-1}.

magnitude, while the Kerr effects for PVF_3, PFM, and PVF_2 are negative, zero, and positive in sign. RIS conformational models have been developed for each of these fluoropolymers,[32] which account for the effects of stereo- and regiosequence for PFM and PVF_3 and PVF_2 and PVF_3, respectively. The $\langle\mu^2\rangle$s calculated for each agree with the experimental values in Table 1, while their ${}_mK$s have not yet been calculated because of the absence of and need for a reliable polarizability tensor for the C—F bond.

PVB Oligomers. The molar Kerr constants and dipole moments of the poly(vinyl bromide) (PVB) oligomers *m*- and *r*-2,4-dibromopentane (DBP) and *mm*-, *mr*-, and *rr*-tribromoheptane (TBH) were measured at room temperature in CCl_4, and both quantities were calculated for each oligomer[25] using two distinct RIS conformational models.[33,34] Both conformational models satisfactorily reproduced the dipole moments and dimensions ($\langle r^2\rangle$) reported for high molecular weight atactic PVBs. Despite the agreement between the dipole moments and dimensions measured for *a*-PVB and the values calculated with either RIS-T[33] or RIS-S,[34] there were notable differences between the two conformational descriptions. Both RIS models found the tg and gt conformations to be preferred for *m*-PVB diads, albeit to different degrees. Though both RIS models also found the tt and gg conformers to be preferred for *r*-diads, RIS-T favored the gg conformer over the tt conformer, while the RIS-S conformational description reversed this conformational preference.

In an attempt to distinguish between these conformational descriptions of PVB, the ${}_mK$s and dipole moments of the PVB model compounds DBP and TBH were measured and calculated using both RIS models.[25] Both individual *m*- and *r*-DBP isomers and DBP and TBH isomer mixtures of *r*:*m* = 58:42 and *rr*:*mr*:*mm* = 38:48:14, respectively, as determined by ^{13}C NMR, were measured. While both PVB conformational descriptions yielded dipole moments in agreement with those measured for DBP and TBH, only the RIS-T conformational model[33] resulted in calculated ${}_mK$s in agreement with those measured for both.

The reason for this behavior can be understood by considering the tt and gg conformations for *r*-DBP, which were found to be energetically preferred by both RIS models. As can be seen in Figure 2, the net dipole moment in the gg conformer lies in the plane of the backbone, which is also the plane of maximum polarizability due to the presence there of both highly anisotropic C−Br bonds. In the tt conformer the C−Br bonds, as well as their net dipole moment, are nearly perpendicular to the backbone. Thus, in the tt conformer the anisotropic C−Br bonds are not in the plane of the backbone and the overall anisotropy of the polarizability tensor is less than in the gg conformer. The tt and gg conformers have nearly identical dipole moments. But because ${}_mK$ is proportional to the vector product of the dipole moment and the direction of maximum polarizability ($\langle\mu^T\alpha\mu\rangle$), the gg conformer has a calculated ${}_mK = 20$, while ${}_mK = 2$ for the tt conformer. In the RIS-S model the tt conformer is preferred over the gg conformer, while the opposite conformational preference is predicted by the RIS-T model. This explains why

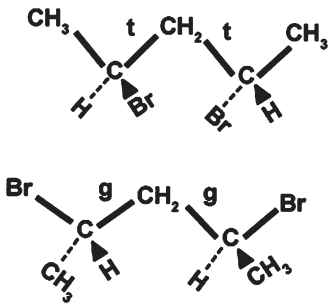

Figure 2. Schematic representation of *r*-DBP in the tt and gg conformations.

${}_mK = 9$ and 15 for *r*-DBP when calculated with the RIS-S and RIS-T models, respectively, compared to the measured ${}_mK = 14$. Since $\mu^2 \sim 6$ D^2 for both preferred conformers, both RIS models yield $\langle\mu^2\rangle = 5.5-5.6$ D^2 for *r*-DBP.

The discrimination and selection among PVB RIS models, afforded by comparison of the molar Kerr constants observed for PVB oligomers to those predicted by them, illustrated once again the high sensitivity of ${}_mK$ to both the conformational and configurational characteristics of flexible polymer chains.

PVC and Its Oligomers. The molar Kerr constants and dipole moments of atactic poly(vinyl chloride) (PVC) and its oligomeric model compounds, *m*- and *r*-2,4-dichloropentanes (DCP) and *mm*-, *mr*-, and *rr*-2,4,6-trichloroheptanes (TCH), were measured in CCl_4 and *p*-dioxane.[23] In addition, ${}_mK$s and $\langle\mu^2\rangle$s were calculated for PVCs and their DCP and TCH oligomers with varying tacticities, using the RIS model previously developed for PVC by Williams, Pickles, and Flory (WPF).[35,36] The measured ${}_mK$s were observed to be particularly sensitive to stereoregularity. For example, *mm*- and *rr*-TCH showed small negative and much larger positive molar Kerr constants, respectively. Comparison with ${}_mK$s calculated using the WPF-RIS model for PVC led to its suggested modification.

Calculated ${}_mK$s were found to be strongly dependent upon the magnitude of nonbonded first-order interactions between Cls and adjacent methine carbons, dependent on the single intervening backbone rotation angle, and second-order interactions between nearest-neighbor Cls, dependent on the pair of intervening backbone rotation angles. The magnitudes of these interactions were modified by making the first-order Cl—CH(Cl) and second-order Cl—Cl interactions less attractive and more repulsive, respectively, than in the WPF-RIS model[35,36] for PVC. The reason for the sensitivity of calculated ${}_mK$s to the repulsive second-order interactions between adjacent Cls is easily demonstrated. For example, in *m*-DCP the tt and g^-g^+ conformations place neighboring −C−Cl bonds closely parallel to each other (see top of Figure 2 and replace *r*-DBP with *m*-DCP), resulting in large ${}_mK$s. Their contributions are necessarily governed by the magnitude of the second-order Cl—Cl interactions.

When this modification of the WPF conformational model for PVC was implemented, dipole moments and ${}_mK$s calculated for atactic PVC and its isomeric oligomers DCP and TCH agreed fairly well with the measured values and also produced calculated dimensions ($\langle r^2\rangle$) in agreement with those[37,38] obtained from intrinsic viscosity−molecular weight measurements performed on PVC fractions in benzyl alcohol.[39] In addition, ${}_mK$s and $\langle\mu^2\rangle$s calculated for PVC were seen to be very sensitive to its tacticity, particularly in both stereoregular regions for ${}_mK$ and in the syndiotactic region for $\langle\mu^2\rangle$.

E−V Copolymers. A series of ethylene−vinyl chloride (E−V) copolymers were produced[40] by the reductive

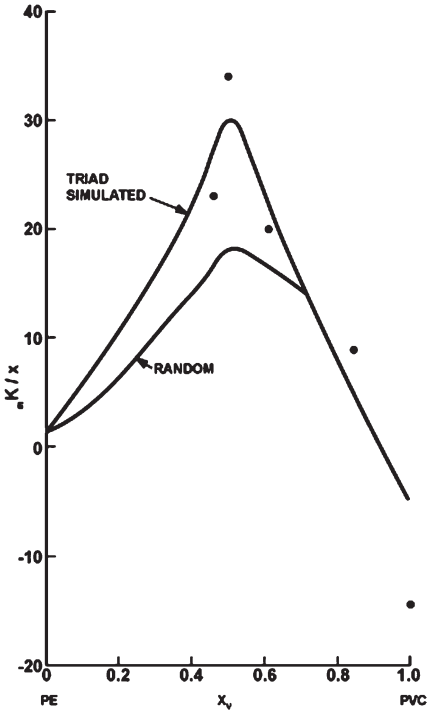

Figure 3. Comparison of observed and calculated molar Kerr constants per repeat unit, $_mK/x$, for E−V copolymers, where X_V is the mole fraction of V units.[41]

dechlorination of PVC with tri-*n*-butyltin hydride [$(n\text{-Bu})_3$-SnH]. Their microstructures (stereosequences and comonomer composition and sequence distribution) were determined by ^{13}C NMR analyses, and SEC/GPC measurements confirmed that all resultant E−V copolymers had the same chain length ($x \sim 1000$ repeat units) as the PVC from which they were obtained. Their molar Kerr constants and dipole moments were measured in *p*-dioxane and compared with those calculated[41] with the RIS model[42] appropriate for E−V copolymers.

When calculating $_mK$s, E−V copolymers were generated by Monte Carlo methods in two different ways. In the first method E and V units were randomly added one at a time with adjacent V units (VV diads) incorporated with a random or Bernoullian probability for meso-diads, $P_m = 0.44$ (44% *m* and 56% *r* VV diads), which corresponded to the stereoregularity of the parent atactic-PVC. The second procedure took cognizance of the detailed E−V microstructures determined experimentally[40] by ^{13}C NMR. For each E−V copolymer we knew its composition, triad comonomer sequence distribution, and the stereosequence of its VV diads. Consequently, each E−V copolymer was generated a comonomer triad at a time to reflect the ^{13}C NMR-observed E−V microstructures. A set of 20 such Monte Carlo generated chains were obtained for each E−V copolymer and used to calculate and average $_mK$s and $\langle\mu^2\rangle$s over this set for both the random and triad simulation methods.

Figures 3 and 4 present the comparison between measured and calculated $_mK$s and $\langle\mu^2\rangle$s, respectively, which are seen to be in agreement. Aside from comonomer composition, it is clear that both the measured and calculated dipole moments are virtually insensitive to E−V microstructure. On the other hand, molar Kerr constants calculated for E−V chains randomly generated and those that were triad simulated to account for their observed commonomer and stereosequence distributions are distinguishable, and the latter are much closer to the measured $_mK$s.

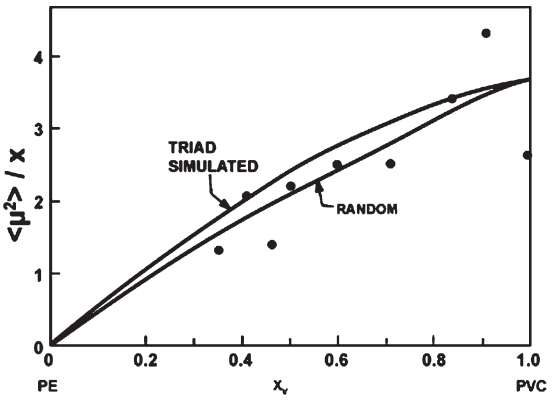

Figure 4. Comparison of dipole moments per repeat unit, $\langle\mu^2\rangle/x$, observed and calculated for E−V copolymers, where X_V is the mole fraction of V units.[41]

As an example, for the E−V copolymer with overall composition $X_V = 0.5$, whose P_m was reduced from 0.44 (PVC) to 0.36, assumption of random chlorine removal during its production leads to a calculated $_mK$ nearly a factor of 2 smaller than is observed. If chlorine removal were a random process, then we would expect all E−V comonomer sequences (VVV, VVE, VEV, EEE, EEV, EVE) to be equally produced, i.e., VVV = VEV = EVE = EEE = 0.125 and VVE + EVV = EEV + VEE = 0.250. Instead, ^{13}C NMR analysis of E−V-50 revealed[40] the following triad distributions: VVV = 0.073, VEV = 0.166, EVE = 0.192, EEE = 0.045, VVE + EVV) = 0.266, and EEV + VEE = 0.258. When $_mK$ is calculated for E−V-50 by triad simulation, which accounts for both $P_m = 0.36$ and the observed comonomer triad distribution, the resulting value is within 10% of the observed molar Kerr constant.

In addition to demonstrating once again the superior sensitivity to microstructures shown by molar Kerr constants in comparison to dipole moments, another more subtle, yet more significant, advantage can be identified. Even in the unusually fortunate case of E−V copolymers produced by the reductive dechlorination of PVC, not all 10 possible comonomer triad sequences could be distinguished and quantitatively determined by ^{13}C NMR.[40] For example, the stereosequences M or R across the central E unit in the V−E−V comonomer triad could not be distinguished. This was only later accomplished[43] through time-of-flight ^{1}H and ^{13}C NMR observations of the $(n\text{-Bu})_3$−SnH reductions of the PVC oligomers *m*- and *r*-DCPs and *mm*-, *mr*-, and *rr*-TCHs. Furthermore, only after these time-of-flight NMR observations was it learned that the $(n\text{-Bu})_3$−SnH reduction of PVC to E−V copolymers was insensitive to microstructures beyond the comonomer triad level. Without this knowledge, it would have been difficult to unambiguously identify/assign their microstructural comonomer and stereosequence triads.

As mentioned previously and seen here for E−V copolymers, even the currently most sensitive means of determining the microstructures of polymers, i.e., ^{13}C NMR observations of their solutions, may not provide microstructural detail at the level that has been observed to influences their molar Kerr constants. This advantage in characterization sensitivity shown by the Kerr effect will now be expanded upon in the following final example, brominated polystryrenes (PSs).

S/*p*-BrS Copolymers. *Kerr Effects of S*/p-*BrS Copolymers with Random Comonomer Sequences*. At the time molar Kerr constants were observed and calculated for random styrene/*p*-Br-styrene (S/*p*-BrS) copolymers,[22] the precise tacticity of the atactic polystyrene (*a*-PS) from which they were obtained

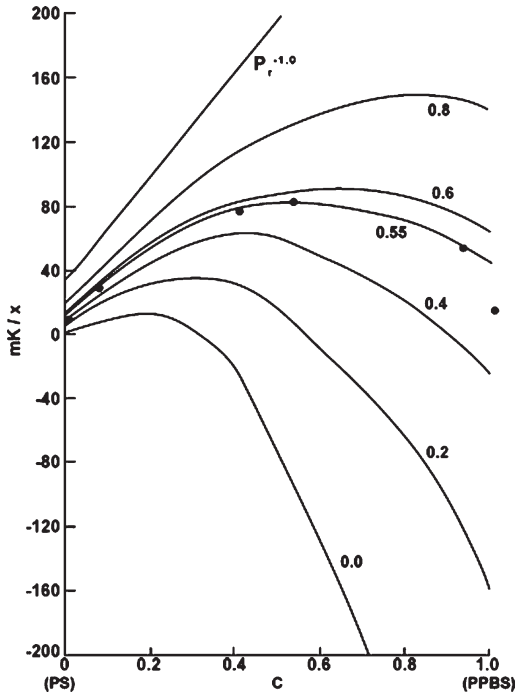

Figure 5. Comparison of $_mK$s observed and calculated for S/*p*-BrS−I copolymers. *x*, P_r, and *C* are the number of repeat units (200), fraction of *r*-diads, and fractional content of *p*-BrS units.[22]

by bromination was unknown and controversial.[44] ^{13}C NMR examinations of *a*-PSs conducted in Japan, Germany, and the US produced considerably different spectra, which were subsequently determined to be due to the solvent sensitivity of their ^{13}C resonances, reflecting the different solvents used by these groups. In response, a series of S/*p*-BrS copolymers with random comonomer sequences were made by brominating the same *a*-PS to achieve different contents of *p*-BrS. Figure 5 presents a comparison of the $_mK$s measured in carbon tetrachloride for these S/*p*-BrS copolymers and those calculated assuming a random (Bernoullian) distribution of comonomer units, but with different tacticities, which were again assumed to have the same random or Bernoullian but undetermined distribution of meso (*m*)- and racemic (*r*)-diads as their parent *a*-PS.[22] This required Monte Carlo generation of a population of S/*p*-BrS chains (15 chains, each of 200 repeat units) corresponding to each overall comonomer composition, with each population generated to have a random distribution of both S/*p*-BrS comonomer units and *m*- and *r*-diad stereosequences.

Note the extraordinary sensitivity of the $_mK$s to both comonomer composition (experimental and calculated) and stereosequence or tacticity (calculated) of the S/*p*-BrS copolymers, which covers a 3 orders of magnitude range and also changes sign. Though not presented here, mean-square dipole moments, $\langle\mu^2\rangle$s, were also measured and calculated for the same S/*p*-BrS copolymers and showed very little dependence on tacticity (calculated), only monotonically increasing with the content of polar *p*-BrS units (experimental and calculated). Like ^{13}C NMR (see below), $\langle\mu^2\rangle$s may be used to characterize only the compositions of S/*p*-BrS copolymers, while $_mK$s can be used to characterize their tacticities as well. The $_mK$s calculated for the complete set of random S/*p*-BrS copolymers assuming a random distribution of 45% *m*- and 55% *r*-diads closely agree with their experimental values, strongly suggesting that the *a*-PS used to generate them has a very similar stereosequence. This was later confirmed by ^{13}C NMR studies performed on the stereoisomeric pentad model compounds of *a*-PS.[45] So, while ^{13}C NMR observations of *a*-PSs could not (without the syntheses of model compounds) determine their tacticities, comparison of measured and calculated $_mK$s for the S/p-BrS copolymers produced from them could.

*Kerr Effects of S/*p*-BrS Copolymers with Variable Comonomer Sequences*. Recently, a second series of S/*p*-BrS copolymers with different contents of *p*-BrS was produced by the bromination of *a*-PS,[46] but in this case variation of their comonomer sequence distributions was attempted. This was achieved by conducting the brominations in solvents that exhibit different qualities for *a*-PS at different temperatures. In this manner the sizes of the randomly coiling *a*-PS chains were varied during the brominations. A family of alkyl chlorides, which have similar small dipole moments,[47−49] but with very different solvent qualities (θ-temperatures) for *a*-PS were employed in the brominations. Kambour et al.[50] had shown that solvents with small permanent dipole moments are capable of polarizing Br_2, enabling its electrophilic substitution/addition exclusively in the *para* position of the phenyl ring of PS without the use of a catalyst.

The θ-temperatures of a-PS in 1-chlorodecane (CD), 1-chloroundecane (CUD), and 1-chlorododecane (CDD) are 6.6, 32.8, and 58.6 °C,[46] respectively. The radius of gyration of a polymer scales with its molecular weight/degree of polymerization *N*, as $N^{3/5}$ (good solvents, $T > \theta$), $N^{1/2}$ (θ-solvents, $T = \theta$), and $N^{1/3}$ (poor solvents, $T < \theta$). As the solvent quality is decreased from good to poor, the macromolecular coil undergoes a transition[51] from expanded coil-to-globule, as depicted in the bottom of Figure 6. Consequently, brominations carried out in CD, CUD, and CDD at 32.8 °C, though proceeding with the same kinetics, should result in the bromination of expanded coils, more compact unperturbed coils, and highly compacted globules of *a*-PS. This should lead to S/*p*-BrS copolymers with different comonomer sequence distributions (see the top of Figure 6), even though each might contain the same over all composition of comonomers.

In Figure 7a the ^{13}C NMR solution spectra of the original *a*-PS and two S/*p*-BrS copolymers each brominated at 33 °C and each with ∼60 mol % *p*-BrS, but one brominated in CD ($T > \theta$) and the other in CDD ($T < \theta$), where the *a*-PS chains should be expanded coils and contracted/compact globules, respectively. Note that the ^{13}C NMR spectra of the two S/*p*-BrS copolymers are virtually indistinguishable and differ only from that of the original *a*-PS by the distinct aromatic carbon resonances of their brominated phenyl rings. If as expected these two S/*p*-BrS copolymers do indeed have distinct comonomer sequence distributions, ^{13}C NMR is clearly unable to confirm this.

By contrast, in part c of Figure 7, the molar Kerr constants measured for *p*-dioxane solutions of three S/*p*-BrS copolymers, each with ∼60 mol % *p*-BrS, but brominated in CD, CUD, and CDD at 33 °C, are clearly distinct. Their Kerr constants are seen to increase in the order S/*p*-BrS (CDD) < S/*p*-BrS (CUD) < S/*p*-BrS (CD), which mimics the increasing solvent quality of their bromination solutions and the expansion of their polymer coils. In Table 2, molar Kerr constants calculated for selected S/*p*-BrS copolymers are presented and compared with the observed $_mK$s. This comparison makes clear that decreasing the solvent quality during bromination of a-PS does in fact lead to a decrease in the randomness and an increase in the blockiness of the resultant S/*p*-BrS copolymers, as their polymer coils contract. Further comparison indicates that the sequence length of *p*-BrS blocks resulting from bromination at 33 °C to the same levels (∼60% *p*-BrS) in CDD and CUD are ∼20 and

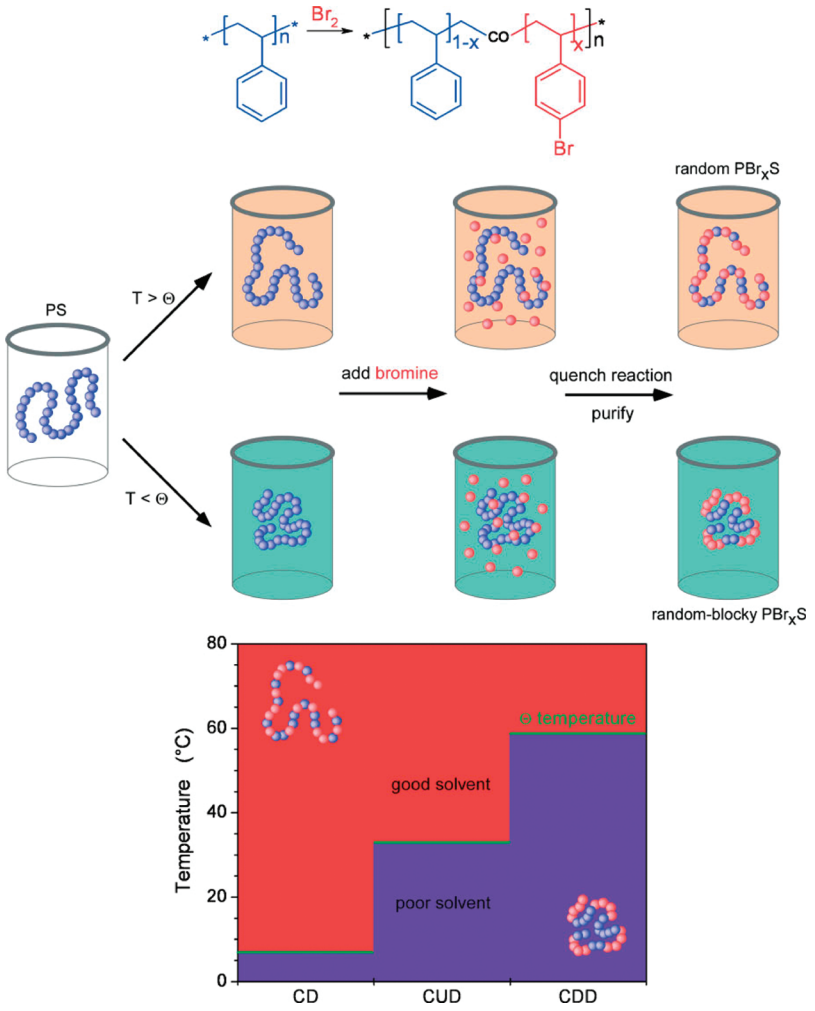

Figure 6. (top) Bromination of polystyrene leading to the formation of poly(styrene-*co*-*p*-bromostyrene). (middle) Parent polystyrene (PS) homopolymer dissolved at room temperature T in either a good solvent ($T > \theta$) or a poor solvent ($T < \theta$), where PS adopts an expanded or collapsed conformation, respectively. (bottom) Depending on the solvent quality, PBrxS copolymers with random (r) or random−blocky (r−b) monomer sequence distributions may be generated.[46]

10 *p*-BrS units, respectively. Thus, we can see that distinctions in comonomer sequence distributions of S/*p*-BrS copolymers between those that are completely random and those that are somewhat and highly blocky can be drawn from the ${}_{m}K$s obtained by measuring the electric birefringence of their dilute solutions. These microstructural distinctions are clearly not visible in their ^{13}C NMR spectra, as is apparent in Figure 7a.

Like their ^{13}C NMR solution spectra in (a), their glass-transition temperatures, T_g, are also insensitive to their comonomer sequences (see Figure 7b). However, though not presented in detail here, it has been demonstrated[46] that films of these S/*p*-BrS copolymers with the same comonomer composition, but with distinct random and blocky comonomer sequences, evidence very different surface dewetting behaviors. Thin films of *a*-PS, *a*-PBr$_{1.0}$S (completely brominated sample), PBr$_{0.59}$S-CD33, and PBr$_{0.58}$S-CDD33 were spun-cast on glass substrates, floated onto deionized water, and transferred onto silicon wafers that were previously decorated with a self-assembled monolayer (SAM) made of semifluorinated 1*H*,1*H*,2*H*,2*H*-perfluorodecyltrichlorosilane (SF) (Figure 8a). After drying, the samples were annealed under a nitrogen atmosphere at $T - T_g = 35$ °C. Dewetting of the copolymer films from the SF-SAM substrates was monitored by optical microscopy. The growth and coalescence of holes in the PS, PBr$_{1.0}$S, and PBr$_{0.6}$S films of various thicknesses were recorded over a period of several minutes to hours (see Figure 8b,c).

The unbrominated *a*-PS films (thicknesses, t, ranging from 68 to 117 nm) dewetted completely from the SF-SAM substrates in a few minutes or less, while films of PBr$_{1.0}$S with comparable thicknesses did not dewet at all. The latter observation suggests that the *p*-BrS units strongly interact with the underlying silica substrates through the thin (≈1 nm) SF-SAM layer. The dewetting rate of PBr$_{0.58}$S-CDD33 thin films is consistently slower than that measured on PBr$_{0.59}$S-CD33 specimens, presumably a consequence of its more blocky character. Thus, the use of Kerr effect measurements to determine their longer-range microstructures has permitted the development of a useful microstructure (comonomer sequence distribution)−property (interfacial response = film dewetting) relation for these copolymers.

As far as I am aware, there exist no other means, including solution NMR, to characterize the microstructures (short- or long-range) of S/*p*-BrS copolymers and, more generally, microstructures beyond those of short-range for most polymers.

It may be worth mentioning that molar Kerr constants calculated for stereoregular S/*p*-BrS copolymers also exhibit sensitivity to their comonomer sequences. For example, ${}_{m}K$s calculated for S/*p*-BrS copolymers containing 60% *p*-BrS

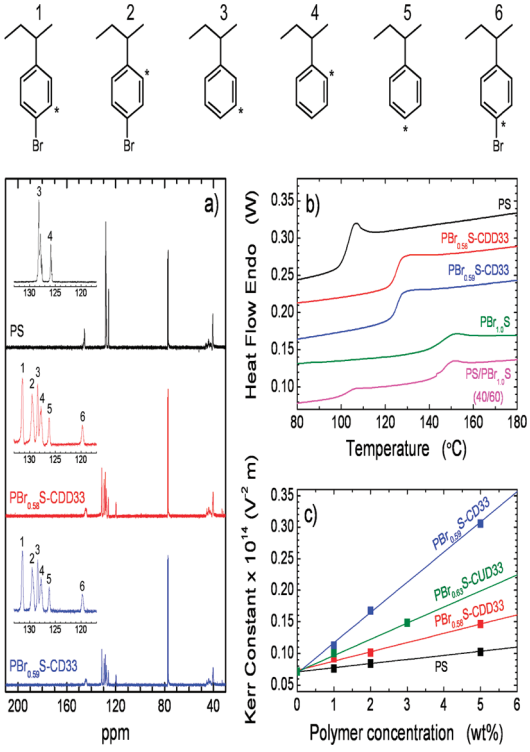

Figure 7. Characterization of poly(styrene-*co*-*p*-bromostyrene) (PBr_xS) copolymers, where x is the mole fraction of *p*-BrS.[46] (a) ^{13}C NMR spectra of PS (top, black line), rb-$PBr_{0.58}S$ (middle, red line), and r-$PBr_{0.59}S$ (bottom, blue line); the peaks in the spectra mark the resonances of phenyl ring carbons in the *ortho*, *meta,* and *para* positions (shown in the upper panel of the figure) in PS and PBr_xSs. The ^{13}C NMR data confirm that the bromination occurred exclusively in the *para* position of the phenyl ring of PS, while the aliphatic part of the PS chain and its ^{13}C NMR spectrum are not affected by the bromination. The mole fraction of *p*-bromostyrene in PBr_xS can be obtained from the ratios of peaks 1 and 3, 2 and 4, or 6 and 5. (b) Differential scanning calorimetry (DSC) from PS (black line), $PBr_{0.58}$S-CDD33 (red line, T = 33 °C), $PBr_{0.59}$S-CD33 (blue line), $PBr_{1.0}S$ (green line), and a mixture of PS and $PBr_{1.0}S$ (40/60 m/m) (magenta line). The DSC results provide the T_g of each material and also serve as further evidence that the bromination reaction takes place on all PS chains present in the reaction vessel. (c) Kerr constant for PS (black line), $PBr_{0.58}$S-CDD33 (red line), and $PBr_{0.59}$S-CD33 (blue line) as measured on solutions (1−5 wt %) of polymers in 1,4-dioxane (> 99% purity) at 293 K.

units may be summarized as follows: (1) For isotactic (i) copolymers, calculated ${}_mK$s are negative and sensitive to comonomer sequence, with much larger values for blocky sequences. (2) For syndiotactic (s) copolymers, calculated ${}_mK$s are only weakly dependent on comonomer sequence, with ${}_mK$(blocky)/${}_mK$(random) ∼ 1. (3) For random comonomer sequences, ${}_mK(s)/{}_mK(a) = 3.2$, ${}_mK(a)/{}_mK(i) = -1.7$, and ${}_mK(s)/{}_mK(i) = -5.4$. Observations (1) and (2) are very distinct from those shown by the atactic S/*p*-BrS copolymers discussed above. These predicted molar Kerr constants suggest the bromination of stereoregular PSs (isotactic and syndiotactic) under different solvent conditions, as described above for *a*-PS, to create stereoregular S/*p*-BrS copolymers with a variety of comonomer compositions and sequence distributions. If these brominations are successful, then the electrical birefringence of their dilute solutions should be observed and their experimental ${}_mK$s determined from them.

Kerr Effect vs NMR. I hope we have successfully demonstrated that polymers containing repeat units that are polar and/or anisotropically polarizable can exhibit molar Kerr constants that are more sensitive to their detailed microstructures than are their NMR spectra. Why then is this the case?

Table 2. Normalized ${}_mK$s for Comonomer Sequence Distributions Calculated Using the PS Rotational Isomeric State (RIS) Model of Yoon et al.[52,22] and Those Experimentally Measured for PBr_xS[46]

monomer sequence distribution	method	${}_mK/{}_mK_{random}$
$(PS_2$-*b*-$PBrS_3)_{60}$	RIS	0.773 ± 0.14^a
$(PS_4$-*b*-$PBrS_6)_{30}$	RIS	0.621 ± 0.14^a
$(PS_{10}$-*b*-$PBrS_{15})_{12}$	RIS	0.363 ± 0.15^a
$(PS_{20}$-*b*-$PBrS_{30})_6$	RIS	0.216 ± 0.15^a
$PBr_{0.63}$S-CUD33	exp	0.533 ± 0.03^b
$PBr_{0.58}$S-CDD33	exp	0.304 ± 0.03^c

[a] Calculated ${}_mK$ for ordered sequence distributions normalized with ${}_mK$ of a random sequence distribution. [b] Experimental ${}_mK$ of $Br_{0.63}$S-CUD33 normalized by the experimentally measured ${}_mK$ of $PBr_{0.59}$S-CD33. The value corresponds to the ratio of the slopes of Kerr constant vs concentration shown in Figure 7c. [c] Experimental ${}_mK$ of $Br_{0.58}$S-CDD33 normalized by the experimentally measured ${}_mK$ of $PBr_{0.59}$S-CD33. The value corresponds to the ratio of the slopes of Kerr constant vs concentration shown in Figure 7c.

A polymer's ${}_mK$ is a "macroscopic" property characteristic of its entire macromolecular chain. Any microstructural element that alters its overall polarizability tensor [$\langle$tr-($\alpha^R\acute{\alpha}^C$)$\rangle$] or changes the magnitude and/or orientation of its overall dipole moment vector with respect to the direction of its maximum polarizability [$\langle\mu^T\alpha\mu\rangle$] will affect its molar Kerr constant. For this reason, the locations of microstructural elements along the polymer chain (middle vs end) may potentially effect either or both the dipolar or polarizabilty terms of a macromolecule's ${}_mK$.

In contrast, NMR, like other spectroscopies, probes the "microscopic" local structures of molecules, including polymers. The resonance frequencies of ^1H and ^{13}C nuclei appearing in the solution NMR spectra of polymers are at best sensitive to short-range microstructural elements, such as the stereosequences of a few consecutive repeat units or the diad or triad sequences of comonomers. This is because the net magnetic fields experienced by them depend solely on their local structural and conformational environments.[2,3]

So while a microstructural alteration anywhere along a polymer chain may be evident in its NMR spectrum, its spectral consequence (chemical shifting of resonances) is not sensitive to nor reflects its position along the chain. Because the molar Kerr constants of polymers depend on the magnitudes and orientations of their overall dipole moment vectors and anisotropic polarizability tensors, identical or similar microstructural alterations located at different positions along the macromolecular chain may potentially produce substantially different changes in the overall ${}_mK$.

The suggested dependence of polymer ${}_mK$s upon the locations, as well as the types, of microstructures along the chain may be illustrated with the following example. Consider the following two atactic S/*p*-BrS triblock copolymers: (I) S_{60}-*p*-BrS_{180}-S_{60} and (II) *p*-BrS_{90}-S_{120}-*p*-BrS_{90}, each with the same tacticity (P_r = 0.55) and comonomer composition (60 mol % *p*-BrS). They differ principally in the locations of their long S and *p*-BrS blocks. This example was not chosen because, as demonstrated above in Figure 7, NMR is powerless to distinguish between them, or for that matter any other similar pair of triblock copolymer with long blocks, but because the conformational characteristics of S and *p*-BrS homopolymers and their copolymers are identical,[52,22] and so their calculated ${}_mK$s are obtained by averaging over the same population of conformations. As a result, any differences in the overall molar Kerr constatnts calculated for each are attributable to the positions/locations/sequences of their long S and *p*-BrS blocks.

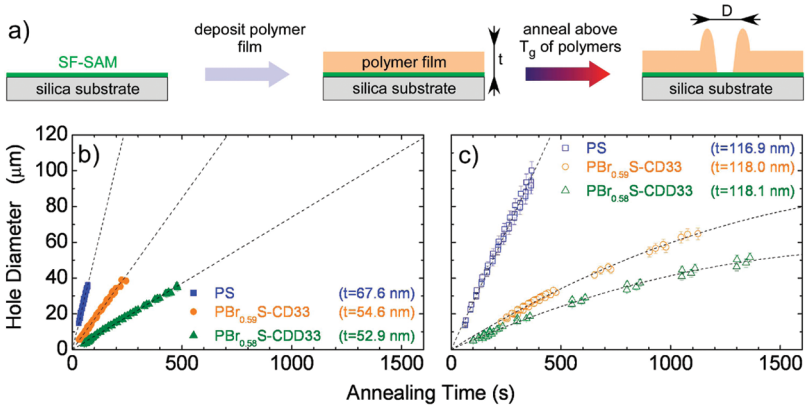

Figure 8. (a) Formation of S/*p*-BrS copolymer film samples for dewetting studies.[46] Upon annealing, holes (diameter *D*) developed in the films and grew with increasing time. The time dependence of the hole diameters for PS (squares), $PBr_{0.59}$S-CD33 (circles), and $PBr_{0.58}$S-CDD33 (triangles) measured on films having a thickness of $t \approx 53-67$ nm (b) and $t \approx 117-118$ nm (c) are presented.

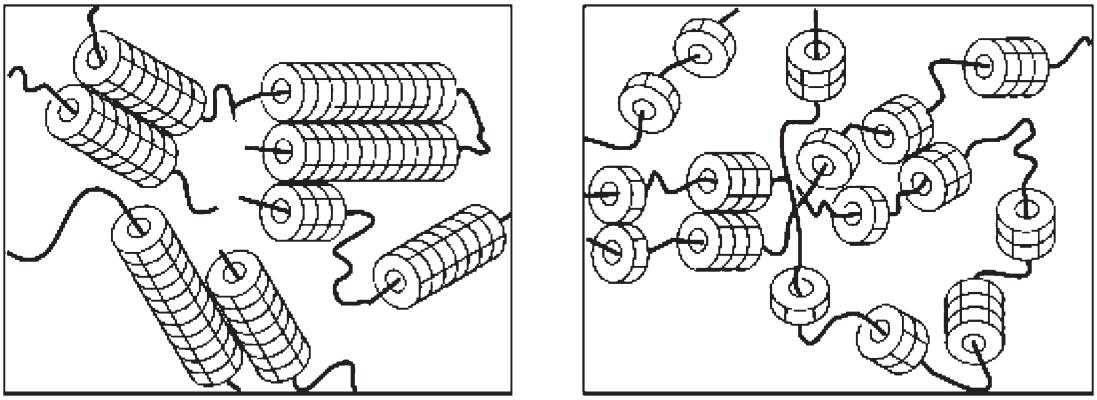

Figure 9. Schematic representation of polymer chains threaded through CDs (right panel). Left panel suggests the beginning of crystallization of threaded CDs.

The calculated magnitude of ${}_mK$(I) is $\sim{}^1/_2$ that of ${}_mK$s(II) and negative in sign, while ${}_mK$s(II) is positive. Both triblock copolymers contain two junctions between their long blocks, and so, they would be indistinguishable by NMR, even if the resonances of their backbone carbons were sensitive to these junctions. Thus, ${}_mK$s are, or may be, superior to NMR as a probe of polymer microstructures because not only can they be more sensitive to the various microstructural types but they may also be sensitive to their locations along the polymer backbone. Even in cases where molar Kerr constants are not as sensitive to polymer microstructures as NMR, unlike NMR, they may still be able to probe their locations along the polymer chain.

Future Potential Kerr Effect Studies of Polymers

Interactions with Small Molecules. Previous experience showed that when PEO was observed in the anisotropic solvent benzene, the ${}_mK$s obtained[30] were much larger than observed[20] in the isotropic solvents CCl_4, *p*-dioxane, and cyclohexane. It was suggested[20] that this was caused by specific solvation/interaction of anisotropic benzene molecules with the PEO chains. Consequently, we suggest and anticipate Kerr effect observations of polymers chemically modified with cyclodextrins (CDs), cyclic starches consisting of 6, 7, or 8 α-1,4-linked glucose units, α-, *β*-, and *γ*-CDs, respectively, following postpolymerization reactions or by threading and noncovalent complexation with polymers.[53] These CD-functionalized polymers, in the first instance, are essentially copolymers containing CDs chemically bound to a certain number of repeat unit side chains. Because in most cases the numbers of CD-derivatized units would be small, and, as for S/*p*-BrS copolymers, NMR would not likely be able to determine the distributions of CD-substituted units, Kerr effect measurements would be undertaken to more fully characterize their substitution patterns.

For polymers that are threaded through CDs to form soluble rotaxanes or pseudorotaxanes (see Figure 9),[53−55] the threaded and noncovalently complexed CDs may or may not be mobile and move along the polymer backbone. Similar to chemical copolymers, the number and distribution of polymer repeat units that reside within the threaded CDs should be sensitively reflected in Kerr effect measurements, especially upon comparison of the ${}_mK$s measured and calculated for the polymers free of and threaded through CDs.

A recent study[54] of poly(ethylene glycol)−α-CD−rotaxanes (r-PEG-α-CD) provides an interesting example. There the diffusion coefficients for PEGs with molecular weights from 3400 to 20 000 Da, and their correspondingly threaded r-PEG-αCDs, with from 50% to 20% of their maximum amounts of α-CDs, were measured. From these observations it was concluded that both the unthreaded PEGs and r-PEG-α-CDs were diffusing as random coils, but with the rotaxanated PEGs exhibiting hydrodynamic radii twice (and presumably dimensions, $\langle s^2\rangle$ and $\langle r^2\rangle$, 4×) those of the unthreaded PEGs. Also, the temperature dependences of their hydrodynamic radii were nearly identical, suggesting that the inherent conformational characteristics of PEG were also dominating the solution behavior of the threaded r-PEG-α-CDs. Dimensions were subsequently calculated[55] for the r-PEG-α-CD formed with PEG (MW = 3400) and

threaded with 14 α-CDs (35% coverage) for various distributions/locations of the threaded α-CDs. Comparison with the dimensions (hydrodynamic radii) observed[54] for the free and α-CD-rotaxanated PEG suggested that the threaded α-CDs tend to cluster in blocks of 3−4 consecutive α-CDs including and covering 6−8 consecutive PEG repeat units.

Because we expect the ${}_{m}K$s of polymer−CD−rotaxanes and −pseudorotaxanes to depend sensitively upon both the numbers and locations of the threaded and polar and polarizable CDs, their observation and study with the Kerr effect seems particularly promising. For example, in the case of the r-PEG-α-CDs mentioned above, we may be able to more sensitively probe the locations (sequence distributions) of threaded and nonthreaded PEG units as well as the orientations of the threaded α-CDs (H-T:T-H, H-T:H-T, etc.) and possibly even their dynamics.

In addition to polymer guests, CDs are able to form soluble rotaxanes and pseudorotaxanes (inclusion complexes) with a large variety of small molecule guests and these have far-reaching industrial applications.[56] In solution a dynamic equilibrium between the included and free guest is maintained. We believe that the Kerr effect examination of dilute solutions formed with host CDs, their small molecule guests, and both simultaneously in nonpolar solvents may provide a sensitive means for not only establishing their equilibrium degrees of complexation but may also be useful for establishing the structures (positions and orientations of guests in the host CD cavities) and host−guest interactions of and in these dynamic noncovalently bonded complexes.

Polymer−Polymer Interactions. As a further potential application of Kerr effect investigations of polymers in solution, it has long been suggested[57−59] stereoregular poly (methyl methacrylates) (*i*- and *s*-PMMAs) in solution adopt nearly all-trans, loosely wound helical conformations over considerable lengths of their backbones. Additionally, when they are mixed in the same solution, they can form a soluble double- or triple-stranded helical stereocomplex, with each *i*-PMMA chain surrounded by one or two *s*-PMMA chains, with different helical pitches, but both with a suggested repeat unit stoichiometry of *s*-PMMA:*i*-PMMA = 2:1. We believe that the ${}_{m}K$s of *i*- and *s*-PMMAs measured in separate and combined solutions, with nonpolar solvents such as benzene and dioxane,[38] and their comparison to ${}_{m}K$s calculated for each and for their complex should provide a sensitive means to characterize their individual and complexed conformations and might possibly indicate their mode of complexation.

Polymers at Interfaces. Finally, an additional class of Kerr effect experiments that might potentially be used to probe the interfacial/surface interactions of polymers can be suggested. Electrodes that are coated with thin films of polymers of one chemical type chemically bonded or strongly adsorbed to the electrode surface at only one end (polymer brushes) can be used to measure the electrical birefringence of solutions made with polymers of the same or a second chemical type. Comparison to Kerr effect measurements performed with bare electrodes may in this manner probe/reflect the interactions between the polymer chains attached to the electrodes and those that are free in solution between the electrodes. The Kerr effects measured for polymer solutions between bare electrodes and those with electrodes coated with a brush of the same polymer, as well as those of a solvent observed with the same bare and polymer brush coated electrodes, can be compared and might serve to probe the natures of the interactions between free and tethered polymer chains and the degree of confinement/extension of the tethered chains, respectively.

In this connection, Lodge and Fredrickson[60] have in fact addressed the optical anisotropy induced by stretching of polymer chains tethered to a surface or belonging to strongly segregated block copolymers that adopt a lamellar phase-separated block morphology. The Kerr effect experiments suggested here may be able to address/assess their conclusions and more generally the characteristics/behaviors of polymer chains confined in brushes and in phase-segregated block copolymers.

It should be mentioned that the suggested Kerr effect measurements performed with electrodes coated with polymer brushes will be anything but routine because the laser beam passing through the Kerr cell will have to sample the solution very near the electrode surfaces in order to probe the attached polymer brushes (see Figure 1). This may be possible by employing a highly focused light beam, a very narrow separation between electrodes, and directing the incoming polarized light beam so that it is repeatedly deflected from and bounces off the electrode surfaces before exiting the Kerr cell. This will require detection of the number of times the light beam is deflected from the electrode surfaces to estimate the total light beam path length in the cell. Calibration could be potentially accomplished by comparison to the Kerr effects measured with bare electrodes using both the straight-through and multiple-deflection light beam modes of operation.

Summary and Request for Polymer Samples

By way of the many examples briefly described above, the molar Kerr constants, ${}_{m}K$, of polymers obtained from the electrical birefringence measured for their dilute solutions have been demonstrated to be, in cases where at least one of their monomer repeat units is polar or reasonably and anisotropically polarizable, exquisitely sensitive to their microstructures, including the tacticities of homopolymers and the comonomer sequences of copolymers. In addition, because the ${}_{m}K$s expected for polymers with given or known microstructures can be estimated if their conformational characteristics have been established, comparison of observed and calculated ${}_{m}K$s can also be used to confirm or derive their conformational models, such as their rotational isomeric states (RIS) models. From such comparisons of observed and calculated ${}_{m}K$s, we were able to conclude that, among all known characterization techniques, Kerr effect studies of dilute polymer solutions are clearly the most sensitive to both their microstructures and their conformations. In addition, ${}_{m}K$s may also be sensitive to the positons/locations of microstructures along polymer chains (middle vs ends) because they depend on their overall dipole moments and anisotropic polarizability tensors.

The recent NSF workshop report on polymers concluded that "recent advances in polymer syntheses leading to elaborate and precise architectures require accompanying advances in microstructural characterization beyond currently available techniques, which are collectively inadequate". We are convinced that the Kerr effect can meet this challenge. Consequently, a call (a plea really) is made to the polymer science community for polymer samples containing polar or reasonably anisotropically polarizable repeat units for further evaluating the Kerr effect as a sensitive means to characterize both their microstructures and conformations. This request is made because of our soon to be achieved and unique capability to measure the ${}_{m}K$s of polymers in solution on a state-of the-art Kerr effect instrument nearing completion in our laboratory, which was prompted by the more than a decade absence in the literature of Kerr effect studies of dilute polymer solutions.

Several additional potential applications of the Kerr effect were suggested for polymers that interact/complex with each

other or with certain small molecules in solution and also for polymers at interfaces, e.g., polymer brushes bathed/swollen in solvents.

Acknowledgment. We are grateful to the Army Research Office for the DURIP award used to build our Kerr effect instrument.

References and Notes

(1) Tonelli, A. E. *Polymers From the Inside Out: An Introduction to Macromolecules*; Wiley-Interscience: New York, 2001; Chapter 8.
(2) Tonelli, A. E. *NMR Spectroscopy and Polymer Microstructure: The Conformational Connection*; VCH: New York, 1989.
(3) Bovey, F. A.; Mirau, P. A. *NMR of Polymers*; Academic Press: New York, 1996.
(4) Tonelli, A. E.; White, J. L. NMR spectroscopy of Polymers. In *Physical Properties of Polymers Handbook*, 2nd ed.; Mark, J., Ed.; Springer: New York, 2007; Chapter 20.
(5) Kerr, J. *Philos. Mag*. **1875**, *50* (337), 416; **1879**, *8* (85), 229; **1880**, *9*, 157; **1882**, *13* (153), 248; **1894**, *37*, 380; **1894**, *38*, 1144.
(6) Briegleb, G. *Z. Phys. Chem*. **1931**, *B14*, 97.
(7) Otterbein, G. *Phys. Z*. **1933**, *34*, 645; **1934**, *35*, 249.
(8) Sachsse, G. *Phys. Z*. **1935**, *36*, 357.
(9) Friedrich, H. *Phys. Z*. **1937**, *38*, 318.
(10) Saiz, E.; Suter, U. W.; Flory, P. J. *J. Chem. Soc., Faraday Trans. 2* **1977**, *73*, 1538.
(11) Nagai, K.; Ishikawa, T. *J. Chem. Phys*. **1965**, *43*, 4508.
(12) Flory, P. J.; Jernigan, R. L. *J. Chem. Phys*. **1968**, *48*, 3823.
(13) Flory, P. J. *Staistical Mechanics of Chain Molecules*; Wiley-Interscience: New York, 1969; Chapter IX.
(14) Flory, P. J. *Macromolecules* **1974**, *7*, 381.
(15) Riande, E.; Saiz, E. *Dipole Moments and Birefringence of Polymers*; Prentice Hall: Englewood Cliffs, NJ, 1992, Chapter 7. However, it should be mentioned that they failed to mention many of the Kerr effect studies my colleagues and I performed prior to 1992, which were performed to determine the sensitivity of the molar Kerr constants of polymers to their microstructures and conformations and which are briefly recapped here.
(16) LeFevre, C. G.; LeFevre, R. J. W. *Rev. Pure Appl. Chem*. **1955**, *5*, 26.
(17) LeFevre, C. G.; LeFevre, R. J. W. In *Techniques of Organic Chemistry*; Weissberger, A., Ed.; Interscience: New York, 1960; Vol. I, Chapter XXXVI.
(18) Tonelli, A. E. *Macromolecules* **1977**, *10*, 153. Also see ref 10.
(19) Kelly, K. M.; Patterson, G. D.; Tonelli, A. E. *Macromolecules* **1977**, *10*, 859.
(20) Khanarian, G.; Tonelli, A. E. *J. Chem. Phys*. **1981**, *75*, 5031.
(21) Khanarian, G.; Tonelli, A. E. *Macromolecules* **1982**, *15*, 145.
(22) Khanarian, G.; Cais, R. E.; Kometani, J. M.; Tonelli, A. E. *Macromolecules* **1982**, *15*, 866.
(23) Khanarian, G.; Schilling, F. C.; Cais, R. E.; Tonelli, A. E. *Macromolecules* **1983**, *16*, 287.
(24) Khanarian, G.; Tonelli, A. E. Nonlinear Optical Properties of Organic and Polymeric Materials; Williams, D. J., Ed.; *ACS Symp. Ser. 233*; American Chemical Society: Washington, DC, 1983; Chapter 12.
(25) Tonelli, A. E.; Khanarian, G.; Cais, R. E. *Macromolecules* **1985**, *18*, 2324.
(26) Tonelli, A. E.; Valenciano, M. *Macromolecules* **1986**, *19*, 2643.
(27) See refs 10, 28, and 29, where it is demonstrated that the polarizability contributions ($\langle \mathrm{tr}(\acute{\alpha}\acute{\alpha})\rangle$) to ${}_{\mathrm{m}}K$s, though generally minor compared with those made by the dipolar term ($\langle \mu^{\mathrm{T}}\acute{\alpha}\mu\rangle$), can be measured independently from the depolarized light scattering of their dilute solutions and also show sensitivity to the microstructures and conformations of polymers.
(28) Tonelli, A. E.; Abe, Y.; Flory, P. J. *Macromolecules* **1970**, *3*, 303.
(29) Suter, U. W.; Flory, P. J. *J. Chem. Soc., Faraday Trans. 2* **1977**, *73*, 1521.
(30) Aroney, M. J.; LeFevre, R. J. W.; Parkins, G. M. *J. Chem. Soc*. **1960**, 2890.
(31) Kuhn, W. *Kolloid-Z*. **1936**, *76*, 258; **1939**, *87*, 3.
(32) Tonelli, A. E. *Macromolecules* **1976**, *9*, 547; **1980**, *13*, 734.
(33) Tonelli, A. E. *Macromolecules* **1982**, *15*, 290.
(34) Saiz, E.; Riande, E.; Delgadp, M. P.; Barrales-Rienda, J. M. *Macromolecules* **1982**, *15*, 1152.
(35) Williams, A. D.; Flory, P. J. *J. Am. Chem. Soc*. **1969**, *91*, 3118.
(36) Pickles, C. J.; Flory, P. J. *J. Chem. Soc., Faraday Trans*. **1973**, *2* (69), 632.
(37) Mark, J. E. *J. Chem. Phys*. **1972**, *56*, 451.
(38) Kurata, M. *Polymer Handbook*, 2nd ed.; Brandrup, J., Immergut, E. H., Eds.; Wiley: New York, 1975; Chapter IV.
(39) Sato, M.; Koshiishi, Y.; Asahina, M. *J. Polym. Sci., Part B: Polym. Phys*. **1963**, *1*, 233.
(40) Schilling, F. C.; Tonelli, A. E.; Valenciano, M. *Macromolecules* **1985**, *18*, 356.
(41) Tonelli, A. E.; Valenciano, M. *Macromolecules* **1986**, *19*, 2643.
(42) Mark, J. E. *Polymer* **1973**, *14*, 553.
(43) Jameison, F. A.; Schilling, F. C.; Tonelli, A. E. *Macromolecules* **1986**, *19*, 2168.
(44) Bovey, F. A. *High Resolution NMR of Macromolecules*; Academic Press: New York, 1972; p 118.
(45) Sato, H.; Tanaka, Y.; Hatada, K. *Makromol. Rapid Commun*. **1982**, *3* (175), 181; *J. Polym. Sci., Part B: Polym. Phys Ed*. **1983**, *21*, 1667−1674.
(46) Semler, J. J.; Jhon, Y. K.; Tonelli, A.; Beevers, M.; Krishnamoorti, R.; Genzer, J. *Adv. Mater*. **2007**, *19*, 2877.
(47) Orofino, T. A.; Mickey, W. *J. Chem. Phys*. **1963**, *38*, 2512.
(48) Orofino, T. A.; Ciferri, A. *J. Phys. Chem*. **1964**, *68*, 3136.
(49) Mays, J. W.; Hadjichristidis, N.; Fetters, L. J. *Macromolecules* **1985**, *18*, 2231.
(50) Kambour, R. J.; Bendler, R.; Bopp, R. *Macromolecules* **1983**, *16*, 753.
(51) Grossberg, A. Y.; Kuznetov, D. V. *Macromolecules* **1992**, *125*, 1970.
(52) Yoon, D. Y.; Sundararajan, P. R.; Flory, P. J. *Macromolecules* **1975**, *8*, 77.
(53) Tonelli, A. E. *Adv. Polym. Sci*. **2009**, in press, and other chapters contained therein.
(54) Zhao, T.; Beckham, H. W. *Macromolecules* **2003**, *36*, 9859.
(55) Tonelli, A. E. *Macromolecules* **2008**, *41*, 4058.
(56) Szejtli, J. *Chem. Rev*. **1998**, *98*, 1743.
(57) Spevacek, J.; Schneider, B. *Adv. Colloid Interface Sci*. **1987**, *27*, 81.
(58) Schomaker, E.; Chella, G. *Macromolecules* **1989**, *22*, 3337.
(59) Kumaki, J.; Kawauchi, T.; Okoshi, K.; Kusanagi, H.; Yashima, E. *Agnew. Chem., Int. Ed*. **2007**, *46*, 5348−5351.
(60) Lodge, T. P.; Fredrickson, G. H. *Macromolecules* **1992**, *25*, 5643.